# Tectonic Evolution of the Sanga Sanga Block, Mahakam Delta, Kalimantan, Indonesia[1]

**Ken McClay,[2] Tim Dooley,[2] Angus Ferguson,[3] and Josep Poblet[4]**

## ABSTRACT

The Sanga Sanga Block contains four large to giant hydrocarbon fields in mid- to upper Miocene deltaic sandstones of the Mahakam Delta, eastern Kalimantan (Indonesia). These fields occur in the northeast-trending Mahakam fold belt, which is characterized by long, tight, fault-bounded anticlines and broad synclines and cored by overpressured shales. Onshore sections of the fold belt are strongly deformed, uplifted, and eroded, whereas the eastern offshore sections are little deformed and buried by the progradational delta wedge. Section balancing of depth-converted seismic lines, together with scaled analog modeling, was used to develop a new tectonic model of inverted delta growth faults for the evolution of the Mahakam fold belt. Section balancing shows that the fault-bounded anticlines of the Sanga Sanga Block are formed by contractional reactivation of early delta-top extensional growth faults. The change from gravity-driven extension to regional contraction occurred at around 14 Ma. Anticlinal folds controlled local sedimentation patterns and influenced the distribution of the reservoir channel sands in the main hydrocarbon fields. Scaled analog models of progradational loading above a ductile substrate produced delta-top extensional growth faults and "depobelts," together with delta-toe fold-thrust. Contraction inverted the extensional growth faults and depobelts, producing tight, fault-bounded anticlines. The results support the model of delta inversion and, thus, the most viable explanation for the geometric, kinematic, and mechanical evolution of the structures in the Sanga Sanga Block. The inverted delta model has applications to other hydrocarbon-bearing deltas around Borneo and in other contracted delta systems.

## INTRODUCTION

The Mahakam fold belt lies within the onshore portion of the Tertiary Kutai Basin on the eastern margin of the island of Borneo (Figure 1). Within this fold belt, the Sanga Sanga production sharing concession (PSC) of VICO Indonesia encompasses four large to giant hydrocarbon accumulations: the Mutiara, Semberah, Nilam, and Badak fields (Bates, 1996), as well as many other smaller fields (Figure 2). Discovered hydrocarbons in the Kutai Basin are estimated to be 2.5 billion barrels of oil (estimated ultimate recovery or EUR) and 28 tcf of gas (EUR) (Paterson et al., 1997). In the Sanga Sanga Block, these oil and gas accumulations occur in a number of long, linear, asymmetric thrust-fault–bounded anticlines in Miocene siliciclastics of the Mahakam Delta system. The anticlines strike north-northeast–south-southwest, range from 2 to 5 km wide, and are typically over 50 km in length (Figure 2), with the fold crests commonly eroded and breached. The anticlines are separated by broad, open synclines (cf. Chambers and Daley, 1997). The western surface expression of the Mahakam fold belt has been termed the Samarinda anticlinorium (Ott, 1987). The lower parts of the Miocene section are strongly overpressured (Bates, 1996), and formerly overpressured shales crop out onshore in the cores of some anticlines (Ferguson and McClay, 1997).

The tectonic origin of the Mahakam fold belt is problematic. Many geodynamic models have been proposed for the formation of this fold belt (cf. Ferguson and McClay, 1997; Chambers and Daley, 1997). Early models postulated that the fold belt



[1]Manuscript received June 16, 1998; revised manuscript received November 12, 1999; final acceptance November 15, 1999.

[2]Fault Dynamics Research Group, Department of Geology, Royal Holloway, University of London, Egham, Surrey, TW20 0EX, United Kingdom.

[3]VICO Indonesia, Jakarta, Indonesia.

[4]Fault Dynamics Research Group, Department of Geology, Royal Holloway, University of London, Egham, Surrey, TW20 0EX United Kingdom. Present address: Departamento de Geologia, Facultad de Geologia, Universidad de Oviedo, C/Arias de Velasco, s/n, 33005 Oviedo, Spain.

Research described in this paper was supported by VICO Indonesia and the Fault Dynamics Research Group, Royal Holloway, University of London. PERTAMINA-VICO and their partners Union Texas Petroleum Limited and Lasmo Indonesia are gratefully thanked for permission to publish. K. McClay also gratefully acknowledges funding from ARCO British Limited. Fault Dynamics Publication No. 87. Critical reviews by G. Eizenstadt, J. McBride, Steve Moss, Neil Hurley, and John Shaw greatly improved the manuscript. April Harper is thanked for help in collation and editing the manuscript. Brian Adams is thanked for the construction and maintenance of the deformation apparatus.

**Figure 1—(a) Plate tectonic setting of southeast Asia showing the location of Borneo and the Mahakam fold belt, Kalimantan (adapted from van de Weerd and Armin, 1992; Hall, 1996). (b) Tectonic map of Borneo showing the location of the Sanga Sanga production sharing concession (PSC).**

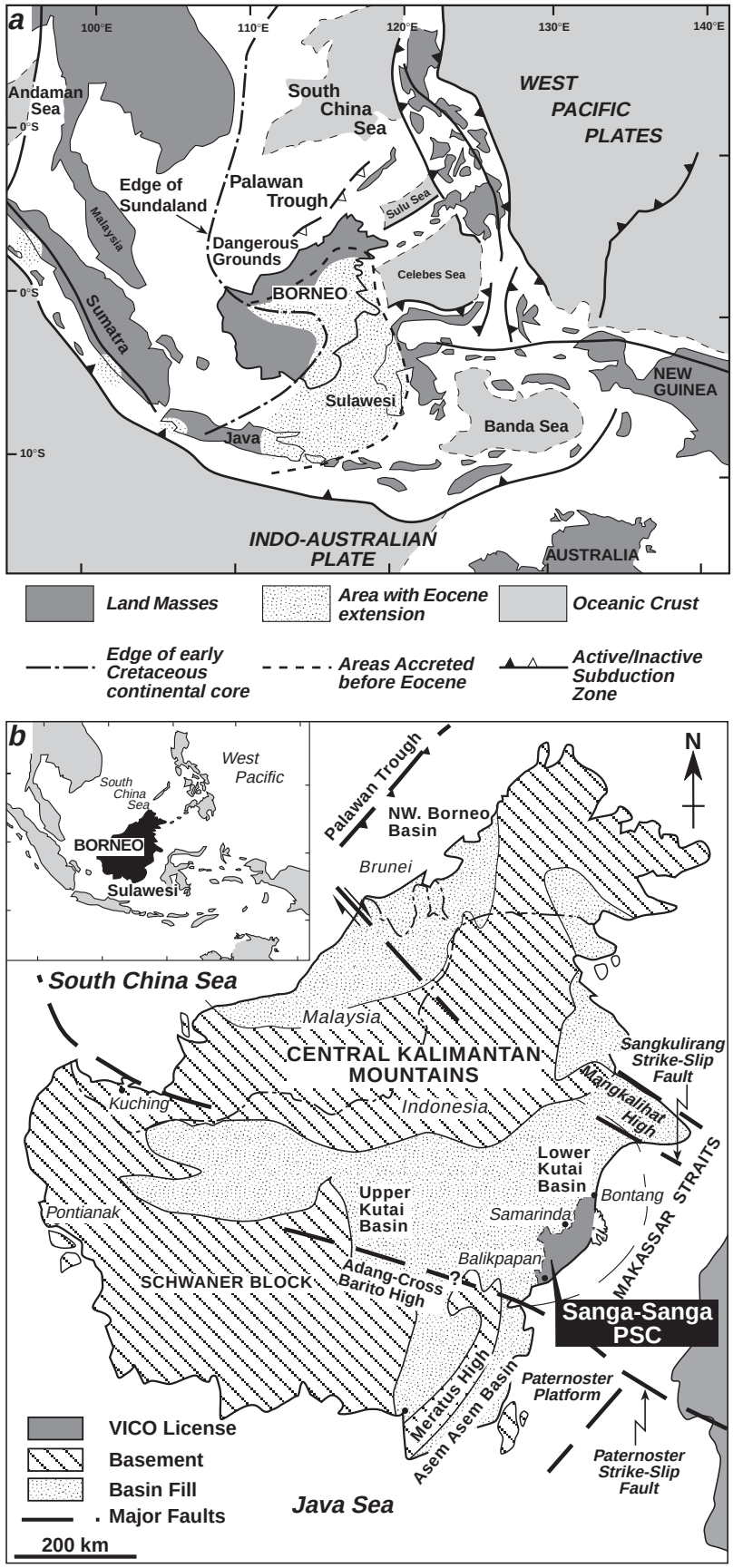

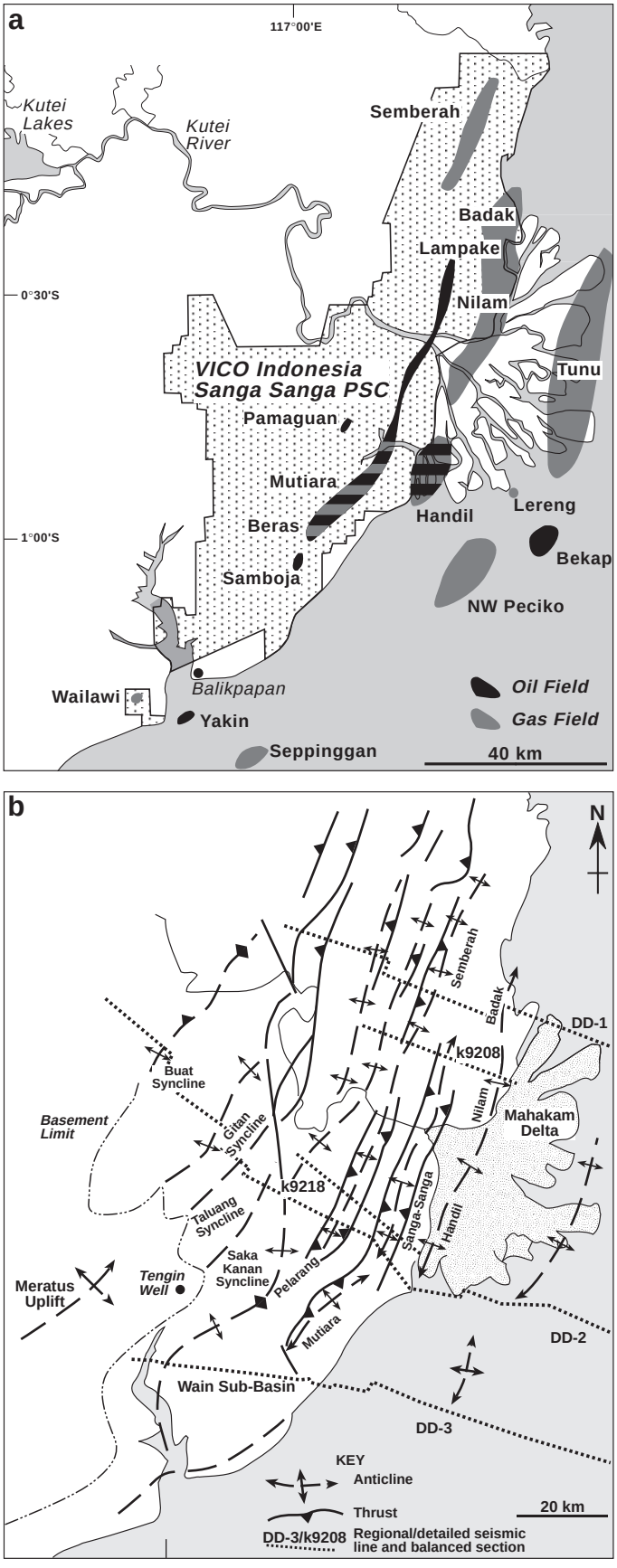


**Figure 2—(a) Map of the Sanga Sanga PSC and the offshore Mahakam Delta system showing the major hydrocarbon accumulations (modified after Bates, 1996). (b) Structure map of the Sanga Sanga PSC showing location of the regional and detailed cross sections presented in this paper.**

was formed by gravity gliding driven by uplift produced by Miocene orogenesis in western Kalimantan, with eastward-vergent collapse of the brittle overburden above overpressured shales (Ott, 1987). Biantoro et al. (1992) proposed a strike-slip–driven inversion model whereby the Samarinda anticlinorium was formed by reactivation of Eocene–Pliocene extensional faults in a restraining stepover between the Paternoster and Sangkulirang strike-slip faults (Figure 1b). The recognition that Miocene contraction uplifted the Upper Kutai Basin and allowed deep erosion (van de Weerd and Armin, 1992) led to tectonic models that involved basement inversion of a deep Paleogene rift basin giving rise to broad regional folding of the overpressured shale section and closely spaced, tight folding in the overlying delta sequences (e.g., Chambers and Daly, 1995, 1997; Cloke et al., 1997, 1999). Other studies have proposed that the Makassar Straits (Figure 1b) was a foreland basin bounded on both sides by foreland fold-thrust belts with the Kutai Basin to the west and the Malene fold belt (Sulawesi) to the east (Bergman et al., 1996). All of these previously proposed models do not adequately account for the structural geometries, timing, and progressive evolution of the Mahakam fold belt in the Sanga Sanga PSC, nor do they allow prediction of structures and reservoirs at depth.

This study stems from a regional geological analysis undertaken by VICO Indonesia from 1992 to 1995, combined with cross section balancing and scaled physical modeling undertaken by the Fault Dynamics Research Group at Royal Holloway, University of London (McClay and Dooley, 1995). We propose a new, integrated tectonic-stratigraphic model for this part of the Kutai Basin and discuss the implications for hydrocarbon generation and accumulation.

## GEOLOGICAL BACKGROUND

### Plate Tectonic Setting of the Kutai Basin and the Mahakam Fold Belt

The tectonic setting of Borneo within the context of the major plates and terranes of southeast Asia has been discussed in detail by Hamilton (1979), Daly et al. (1991), van de Weerd and Armin (1992), Hall (1996, 1997), Metcalfe (1996), Packham (1996), and Longley (1997). Only a brief overview will be presented here. Interactions of the Philippine Sea plate, the Indo-Australian plate, and the Eurasian plate since the Cretaceous have generated a complex assemblage of small marginal ocean basins and microcontinental blocks bounded by subduction zones, extensional margins, and major transcurrent faults in the Indonesian region (Figure 1a). The island of Borneo, and in particular the Kutai Basin and the Mahakam fold belt, have experienced a complex tectonic history from the Paleogene to the present day (e.g., Moss et al., 1997; Cloke et al., 1999; Moss and Chambers, 1999).

The basement of the Kutai Basin is probably an Upper Cretaceous assemblage of microcontinental fragments, ophiolites, and accretionary prism sediments intruded by Cretaceous plutons (Moss et al., 1997). These units crop out around the basin margins in the Central Kalimantan Mountains to the north and northwest, and in the Schwaner Block to the west (Figure 2a). Middle Eocene to early Oligocene rifting (probably as a southwestward extension of the opening of the Celebes Sea) produced a series of east-dipping extensional fault systems that formed half grabens infilled with continental to marine clastics (Moss et al., 1997). In the late Oligocene, there is evidence of a regionally important contractional deformation and uplift in the western parts of the Kutai Basin (cf. Moss et al., 1997; Chambers and Daley, 1997).

The early Miocene–middle Miocene was a period of major plate readjustments with the rotation of Borneo (from 20–10 Ma) (Hall, 1996, 1997). This resulted in deformation and uplift of Borneo and a major influx of volcanogenic clastics into the Kutai Basin from the uplifted terranes to the west. Collision of microcontinental blocks with a subduction zone along the northwest Borneo margin (Palawan Trough) resulted in uplift that produced the Central Kalimantan Mountains. In the Sanga Sanga area, this coincides with the lower Miocene shelf sandstones and carbonates becoming overlain by middle to outer shelf shales, which, in turn, were covered by progradational sandstones and shales of the Miocene Mahakam Delta system.

The early middle Miocene (~14.0 Ma) marks the start of the main period of basin inversion in the Sanga Sanga area (Ferguson and McClay, 1997). The deformation migrated progressively from the west to the east with dominantly east-vergent inverted faults coupled with eastward migration of basin depocenters. At the middle–late Miocene boundary (10.5 Ma), a pronounced eastward shift of depocenters and accelerated inversion can be attributed to the Banggai-Sulu collision in Sulawesi east of the Kutai Basin (cf. Moss et al., 1997). The early Pliocene (6.5 Ma) marked continued structural inversion and progressive eastward shift of depocenters. Pliocene–Pleistocene inversion and uplift of the Meratus Mountains south of the Kutai Basin indicate continued regional contraction at this time. In the Mahakam fold belt, late tightening and thrusting occurred within the anticlines of the Sanga Sanga Block. This major phase of contractional tectonics is interpreted to be the result of the collision of the Indo-Australian plate with the Banda arc (Daly et al., 1991; van de Weerd and Armin, 1992). Throughout the inversion history of the Kutai Basin, from the

middle Miocene to the present day, the dominant shortening direction was to the northwest as deduced from the relative plate motions, from the trend of the major fold structures observed both onshore and offshore, and from borehole breakout studies in the Kutai Basin (Ferguson and McClay, 1997; Syarifuddin and Busono, 1999).

### Stratigraphy of the Kutai Basin

The Kutai Basin is the deepest Tertiary basin in Indonesia, having accumulated over 14 km of sediment. It is bounded by the Paternoster platform, Barito Basin, and the Meratus Mountains to the south, by Schwaner Block to the southwest, the Mangkalihat high to the north-northeast, and the Central Kalimantan Mountains (Moss and Chambers, 1999) to the west and north (Figure 1b). The Kutai Basin is subdivided into the Upper Kutai Basin, consisting of Paleogene outcrops with Cenozoic volcanics possessing a strong northwest-southeast structural grain, and the Lower Kutai Basin with Miocene strata cropping out in north-northeast–trending structures. The Meratus Mountains to the southwest and the Central Kalimantan Mountains to the north of the Kutai Basin have an ophiolitic basement together with Paleogene strata striking dominantly in a north-northeast direction (Figures 1, 2). The Sanga Sanga PSC occurs in the onshore part of the Lower Kutai Basin located between Balikpapan and Bontang (Figures 1, 2).

The producing fields in the Sanga Sanga PSC are located on the north-northeast–trending structures of the Mahakam fold belt. The largest hydrocarbon accumulations occur along a simple north-northeast–trending anticlinal structure from Badak in the north to Nilam and Handil in the south (Figure 2b). The hydrocarbons are trapped in middle and upper Miocene deltaic sandstone reservoirs that occur mainly in four-way dip closures or two-way structural/stratigraphic traps that result from delta-plain, reservoir-channel sandstones crossing a later structural high at an oblique angle.

Figure 3 shows a chronostratigraphic chart for the Sanga Sanga Block, Kutai Basin. In the Lower Kutai Basin, clastic deposition has occurred almost continuously from the middle Eocene (synrift), through the Oligocene (postrift), to the present-day recording eastward progradation of the Mahakam Delta system. As a result, there has been a progressive eastward migration of the basin depocenter (Figure 3). Uplift and removal of section (particularly focused on the anticlines) (Figure 3) has occurred progressively from west to east as a result of the middle Miocene to present-day contraction that produced the Mahakam fold belt.

The Mahakam Delta system deposited up to 3 km of sand, shale, and coal-rich sequences in the proximal deltaic facies and an underlying thick, shale-dominated sequence in the distal marine prodelta facies (Figure 3). Sedimentation rates are calculated to average approximately 1000 m/m.y. (decompacted) (Bates, 1996). Overpressuring, largely due to compaction disequilibrium (Bates, 1996) and organic maturation, occurs at depths of 2–4.5 km throughout the Kutai Basin and underlies the fold belt, giving rise to poor seismic imaging at depth (Bates, 1996; Paterson et al., 1997). The overpressures occur predominantly in the fine-grained clastics deposited in distal deltaic and deeper marine environments (Bates, 1996).

### Structure of the Mahakam Fold Belt

The Mahakam fold belt is characterized by tight, asymmetric anticlines separated by broad synclines in Miocene strata (Figure 2). The axial traces of these structures are long (20–50 km in strike length) and linear to gently curved (Figure 2). Figure 4 shows three regional, balanced, composite cross sections across the Mahakam fold belt. The fold belt is characterized by detachment-style folds that change from simple symmetric/asymmetric structures in the easternmost region, to lift-off folds, to thrust-cored folds in the central zone, and into a detached fold belt in the western part of Kutai Basin (Figures 4, 5). Greater uplift and resultant erosion in the western area reveals more complex fold patterns at deeper levels. The western part of the cross sections in Figure 4 shows the complex, faulted folds of the Buat, Gitan, Taluang, and Saka Kanan synclines. In contrast, the eastern part of the Mahakam fold belt in the Sanga Sanga PSC shows more open anticlinal structures with minor reverse/thrust faulting (Figure 5). These eastern anticlines trap the major hydrocarbon accumulations in the Sanga Sanga PSC (Figure 2).

## RESEARCH METHODOLOGY

The structural analysis of the Mahakam fold belt has involved interpretation of over 10,000 km of two-dimensional seismic data and over 600 wells drilled on the Sanga Sanga PSC. Key regional horizons were identified in wells and were mapped over the PSC using the seismic data. Horizons were labeled using an alphabetic "in-house" VICO nomenclature (Figures 3, 4) and tied to biozones using foraminifera biostratigraphy.

### Cross Section Balancing and Restoration

Three composite regional and six detailed cross sections were constructed, balanced, and sequentially

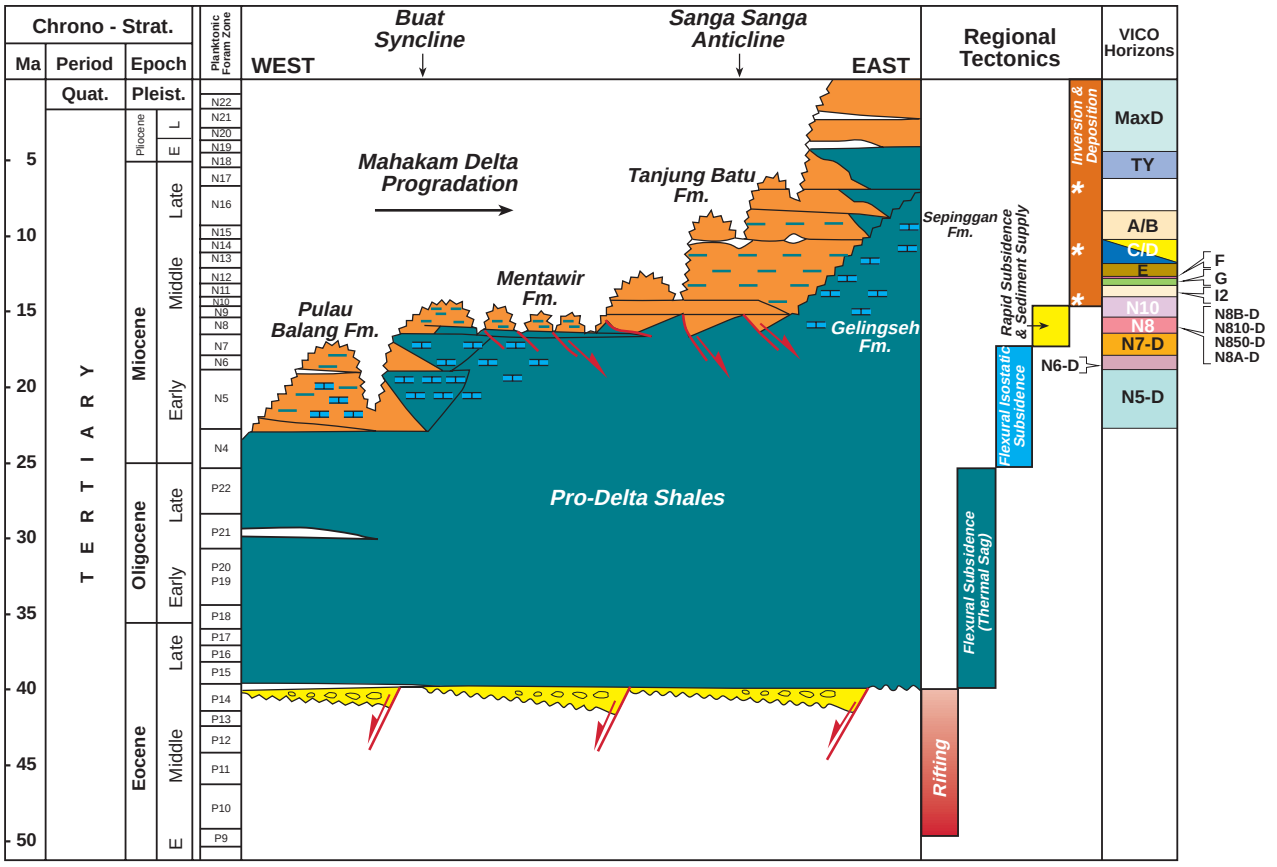


**Figure 3—Summary chronostratigraphic chart for the Sanga Sanga PSC. Data from this study and VICO Indonesia.**

restored using the computer section balancing software GEOSEC™. Cross sections constructed from depth-migrated seismic sections integrated with well data were used to determine the timing of structural development and to calculate the amounts of uplift and shorting at particular time horizons. Of the main algorithms that may be used to geometrically restore cross sections (Williams and Vann, 1987), bed-parallel flexural slip gave the best results and produced geologically reasonable surface fold geometries that could be matched with geologically reasonable fault shapes in the subsurface. The cross sections presented in this paper (Figures 4, 5) thus were sequentially restored using the flexural slip algorithm (note, however, that this gives minimum values for the extensional deformation). The sequentially restored cross sections were used to determine the timing of structural development and to calculate the amounts of uplift and shorting at particular time horizons. In addition, uplift data based on velocity analyses and vitrinite reflectance data (Grundy et al., 1996) were incorporated into the section balancing of the Max D surface (Figures 4, 5).

## Scaled Physical Modeling

Scaled physical models, designed to simulate differential sedimentary loading and inversion in a progradational delta system, were constructed in a deformation rig 60 cm wide and 1.0–1.5 m long (Figure 6). The overpressured muds at the base of the simulated delta section were modeled using a viscous silicone polymer layer, and the overlying delta sediments were simulated using dry, nearly cohesionless granular materials, such as quartz sand and glass beads. A uniform, 1-cm-thick basal layer of silicone polymer (Dow Corning SGM-36™) (Weijermars et al., 1993) was overlain by a 0.5–1.0-cm-thick, predifferential load layer of dry, silica sand (grain size 190 μm) that was mechanically sieved into the rig. The polymer layer was confined by the end walls of the apparatus (Figure 6a). Experiments were done both with a basal 2° slope and without a slope at the base of the model. Differential sedimentary loading produced by delta progradation was simulated by mechanically layering a 2.0–2.5-cm-thick wedge of alternating colored sand layers (2–3-mm-thick individual layers) on top

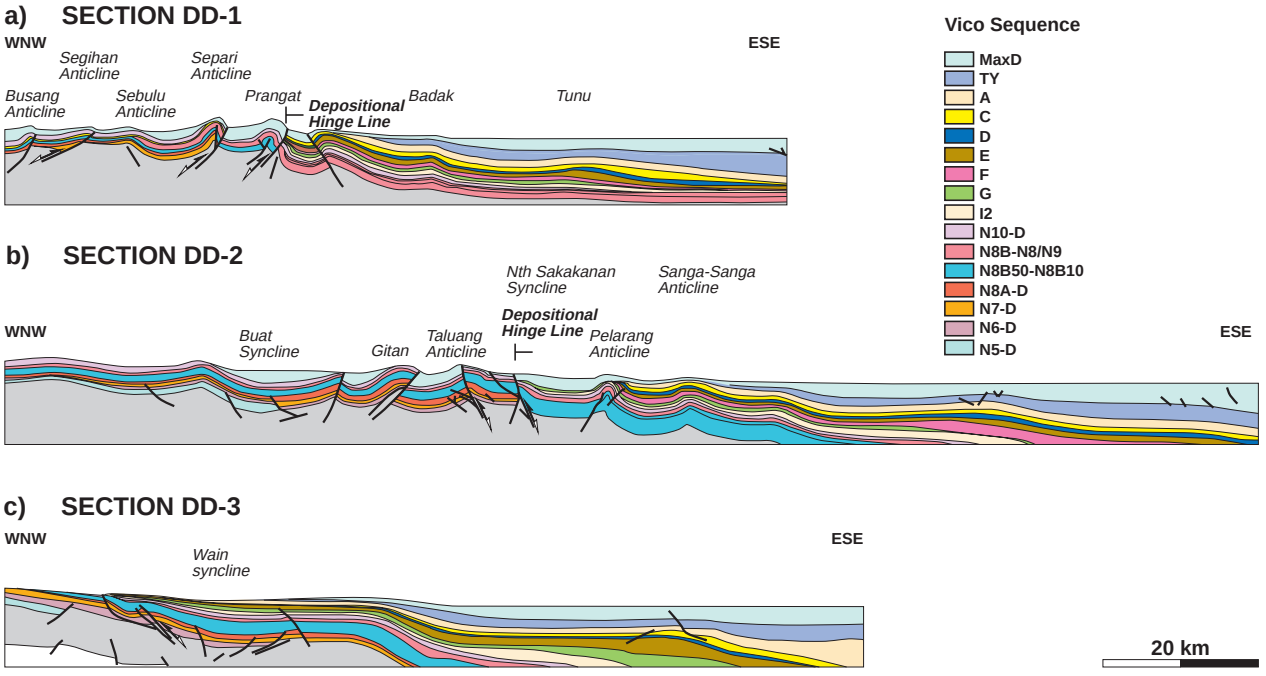


**Figure 4—Regional balanced cross sections for DD-1, DD-2, and DD-3 across the Sanga Sanga PSC. The locations of these regional lines are indicated on Figure 2b.**

of the prekinematic assemblage of polymer and sand layers at the base of the rig (Figure 6b). In single differential load experiments, the model was then allowed to deform under its own weight over a period of up to 24 hr (see McClay et al., 1998). The differential load between the sand wedge and the unloaded section of the model results in flow of the viscous polymer from underneath the sand wedge to the front of the model, producing a "delta-toe" fold-thrust belt. The resultant "delta-top" graben systems were infilled with synkinematic sand layers after each 0.5–1.0 cm of delta-top extension. Double differential load models were constructed by placing a second differential load outward over the first load (Figure 6b), such that the initial delta-toe fold belt was buried by the second progradational load. After this second loading stage, the models were again allowed to deform under their own weight for further periods of up to 24 hr. As in the single differential load experiments, the second-phase delta-top graben systems were infilled with synkinematic sand layers after each 0.5–1.0 cm of delta-top extension.

The models were inverted by moving the left end wall of the deformation rig inward via motor-driven worm screws at a strain rate of $1 \times 10^{-4}$/s such that the sandpack was contracted under a horizontal maximum compressive stress. At the end of deformation, the models were filled to the top with a postkinematic sand layer so that they could be preserved by impregnating with a gel and serially sectioned for detailed internal analysis. The progressive deformation of each model was recorded by 35 mm time-lapse photography.

The models are dynamically scaled such that 1 cm in the model approximates to 1 km in the crustal prototype [see detailed discussions on model scaling in Brun et al. (1994), Weijermars et al. (1993), and McClay (1990)]. The models were constrained at the right end wall (Figure 6). In the natural prototype, this lateral constraint occurs at the end of the overpressured zone, such that it provides a buttress against which the delta-toe fold and thrust belt develops.

In the course of this research program, 15 experiments involving both single and multiple differential sedimentary loading of a ductile substrate, together with subsequent contraction and inversion, were run. McClay et al. (1998) summarized models involving single and double differential loads without contraction, and Ferguson and McClay (1997) summarized the results of analog models that tested the viability of previously proposed geodynamic models for the Mahakam fold belt (e.g., thin-skinned contractional tectonics, basement-involved extension and subsequent inversion, coupled strike-slip faulting, downslope gravitational gliding, and

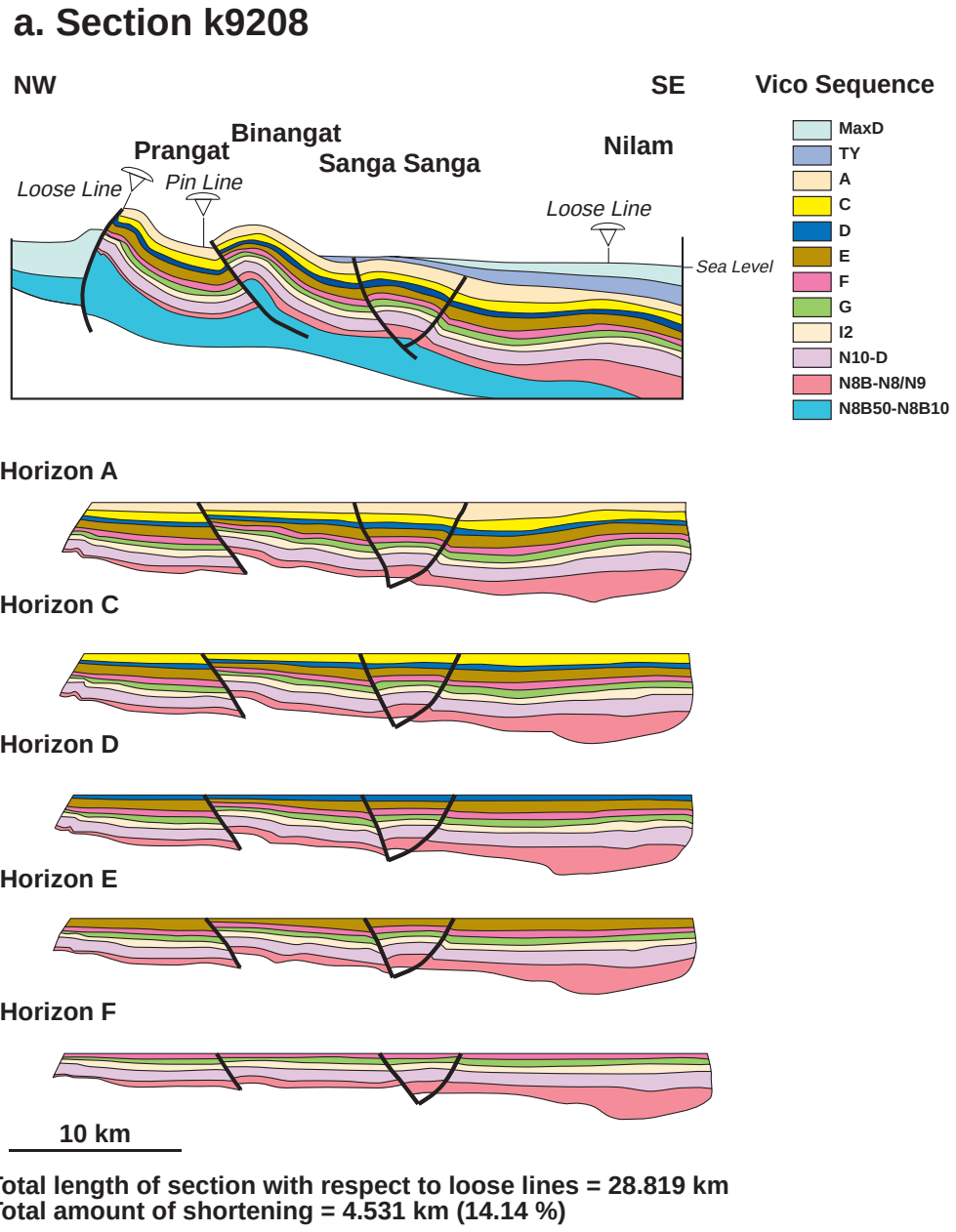


**Figure 5—Balanced and restored detailed seismic sections (a) k9208 and (b) k9218 across the Mutiara field. Locations of these seismic lines are shown on Figure 2b.**

simple differential loading without inversion). Ferguson and McClay (1997) concluded that none of these models adequately accounted for the geometric and kinematic evolution of the Mahakam fold belt in the Sanga Sanga PSC. In contrast, models that combined differential (delta) loading with inversion resulted in structures that showed strong geometric and kinematic similarities to those in the Mahakam fold belt in the Sanga Sanga PSC. These results are summarized in the following sections.

## RESULTS

### Cross Section Balancing

Figure 4 shows three composite regional balanced cross sections across the Mahakam fold belt. The western onshore part of sections DD-1 and DD-2 shows strong folding with tight, fault-bounded anticlines and broad synclines (Figure 4). In contrast, the eastern part of these cross sections and section DD-3 across the Wain subbasin are only

Figure 5—Continued.

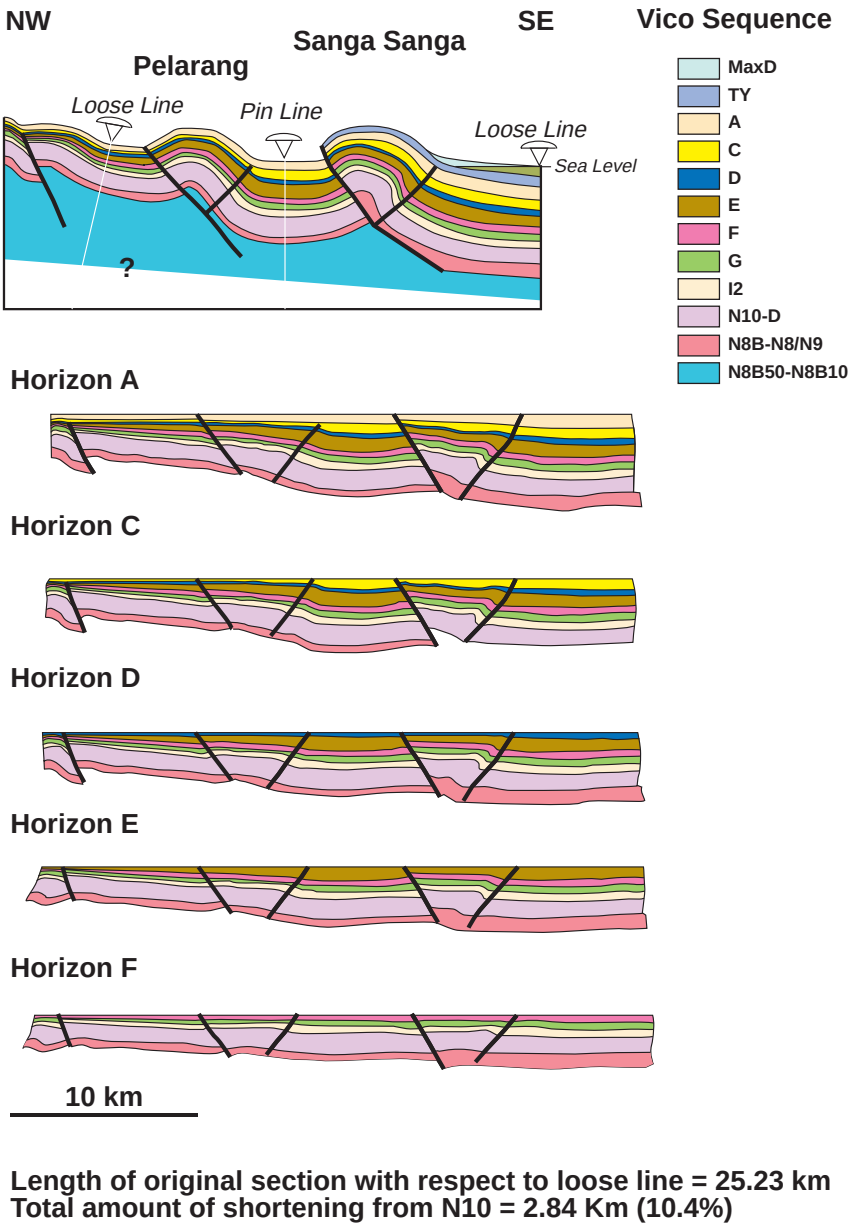


gently folded with the folding decreasing to the east. Here, the strata are typically delta-slope deposits that generally dip and thicken eastward into the Makassar Strait Basin (Figure 4). On each cross section there is a hinge line that delineates marked uplift to the west and overall subsidence to the east (Figure 4).

Many of the major faults that bound the anticlines on the cross sections show thickness changes across them in the lower Miocene from sequences N4-N5D to N8/N9. Sequential restorations of these cross sections show that these faults were extensional at least over this period and were reactivated in contraction at around the time of N10D deposition. For the western parts of sections DD-1 and DD-2, 5 and 5.2 km of extension, respectively, have been calculated. In contrast, cross section DD-3 shows only 2.1 km of extension (McClay and

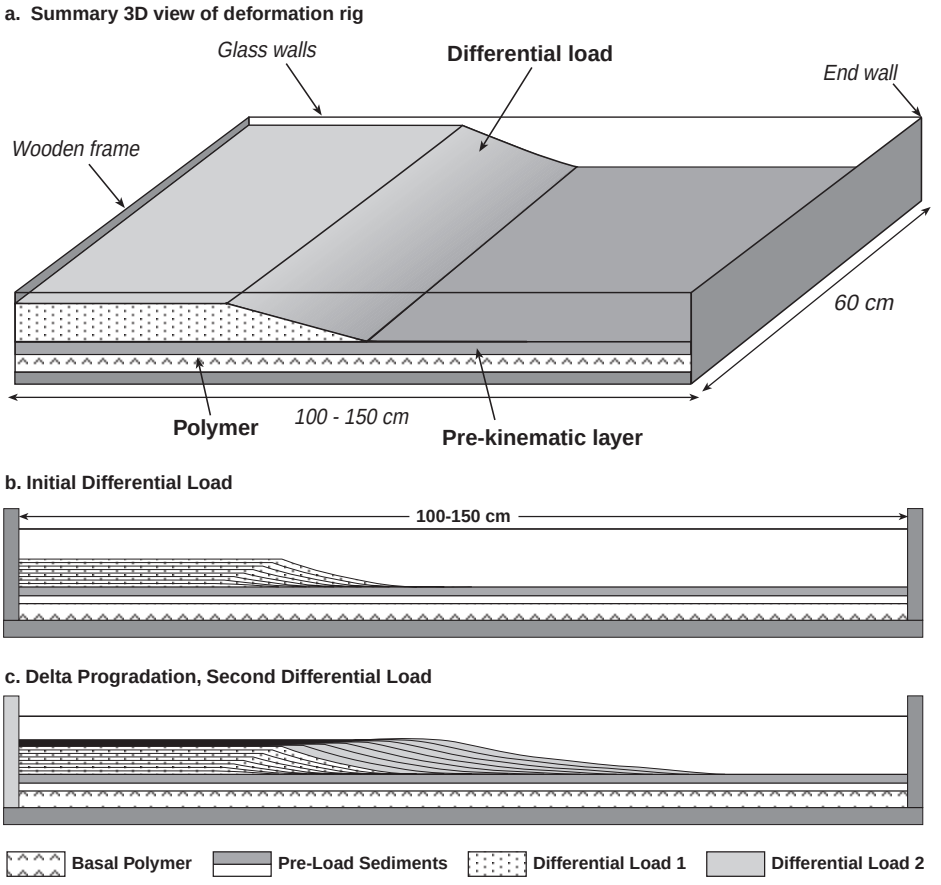


**Figure 6—(a) Three-dimensional view of the deformation apparatus used during this study. (b) Cross section view of a typical analog model after an initial differential load (progradational delta wedge) is placed on the mobile substrate. (c) Cross section view of the model after major progradation of the delta wedge.**

Dooley, 1995). Extension occurred on both regional, east-dipping, down-to-the-basin faults and counterregional, west-dipping, landward faults.

Shortening began during N10 deposition (~14 Ma, middle Miocene) and continued to the present day. Section DD-1 underwent 7.4 km of shortening, section DD-2 had 8.7 km of shortening, and section DD-3 underwent only 0.9 km of shortening (McClay and Dooley, 1995). Most of the shortening focused in the western parts of the sections (Figure 4) where reactivation of the extensional faults produced uplifted, tight, fault-related inversion anticlines. These are now strongly eroded with removal of most or all syncontractional strata. The Max D surface is an estimation of the amount of section removed by erosion (Grundy et al., 1996). There is a minimum of 1 km of uplift on the western part of section DD-1 and 1800 m of uplift in the Buat syncline on section DD-2 (Figure 4). Significant uplift is also seen on the western end of section DD-3. East of the hinge lines, the amount of folding is significantly less and progressively decreases eastward (Figure 4).

Six detailed sections were restored across the Sanga Sanga PSC, two of which are shown in Figure 5. Line k9208 crosses the Prangat, Binangat, and Sanga Sanga anticlines and extends to the Nilam anticline (Figure 5a). Sequential restoration shows that the Sanga Sanga and Binangat anticlines developed on preexisting extensional fault systems. A total of 1.31 km (4.1%) of extension occurred until N8–N10 deposition, forming a local depobelt bounded by regional and counterregional extensional faults. Since N10 deposition, the section has undergone a total of 4.53 km (14.14%) of contraction up to the present day (Figure 5a). At the early stages of contraction the shortening was accomplished by reactivation of the extensional faults (from N10 to A deposition). Most of the shortening was accommodated by the formation of fault-related folds (Prangat, Binangat, and Sanga Sanga) late in the tectonic evolution, from horizon A deposition to the present day (Figure 5a). Internal deformation and buttressing are shown in this section by the overturning of the reverse fault (formerly a regional fault at N8 deposition) at Prangat (Figure 5a).

Figure 5b shows a detailed cross section through the Pelarang and Sanga Sanga anticlines on seismic line k9218. In this section extension can be recognized

from N8 deposition until N10 deposition with a total of 0.95 km (3.47%) of extension. This deformation occurred on extensional faults in the positions of the Sanga Sanga and Pelarang anticlines (Figure 5b). Contraction occurred after N10 deposition by the reactivation of the extensional faults and continued to the present day. Initial inversion appears to produce reverse slip and gentle hanging-wall folding on the reactivated extensional faults. Most of the shortening occurred after horizon A deposition, with the development of fault-related folds in the hanging walls of the reactivated extensional faults (Figure 5b). From the time of deposition of horizon C (10.5 Ma) until the present day, the main focus of inversion has been on the regional fault beneath the Sanga Sanga anticline (Figure 5b). The amount of shortening from N10 deposition (14.0 Ma) to the present day is 2.8 km (10.6%), indicating a net contraction of the cross section.

The section balancing and sequential reconstructions have validated that the cross sections are geometrically and kinematically admissible. The regional cross sections indicate that extension took place mainly by both regional and counterregional growth faulting and that these faults are now localized in the cores of the present-day anticlines. The change from an overall extensional regime to a contractional regime started during N10 deposition (~14.0 Ma). After N10 deposition to present-day contraction produced inversion by reactivation of older extensional faults, together with late-stage formation of hanging-wall fault-related folds.

## Scaled Physical Modeling

The detailed results of a representative analog model that underwent two periods of differential loading (simulating two phases of delta progradation) followed by inversion/contraction are presented in the following section. Although only the results of one model are presented in full, similar features have been found in many repeat experiments. Thus, two other models that show structures relevant to the evolution of the Mahakam fold belt are also presented.

Figure 7a illustrates the model after 5.0 hr with a single differential load. A delta-top graben is well developed and consists of segmented regional and counterregional extensional faults parallel to the slope break (shelf edge). This forms a localized depobelt that was incrementally infilled with synextensional sand layers. Extension on the delta top was balanced by the formation of a fold-thrust belt at the toe of the progradational load. Ductile polymer at the base of the model has migrated forward under the differential load to give extension on the delta top and contraction at the toe. In the second stage of this model, a second differential load was introduced covering the first-stage graben and fold-thrust systems (Figure 7b). A second delta-top graben system formed directly on top of the first-phase fold-thrust belt, together with a second fold-thrust belt at the delta toe (Figure 7b). After another 2.5 hr of deformation under the second differential load, the model was covered by postextension, preinversion glass beads and sand layers. It was then contracted a total of 10 cm by moving the left end wall inward (Figure 7c). Contractional deformation produced synchronous reverse reactivation of the extensional faults that bound both the phase 1 and phase 2 graben systems to produce broad, boxlike anticlines in the postextension sequence (Figure 7c). The second-phase fold-thrust belt at the toe of the sand wedge was visibly amplified as polymer migrated into the cores of the folds (Figures 7c). A thin syninversion sequence of sand layers was added incrementally as contraction progressed to simulate syninversion delta sedimentation. In addition, a steep reverse fault system formed on the left side of the model (Figure 7c) as a result of buttressing against the left end wall. The contractional deformation produced inversion anticlines bounded by reactivated faults above both the phase 1 and phase 2 extensional graben systems (Figure 7c, e). These features are clearly seen in the three-dimensional reconstruction of this model shown in Figure 8.

Figure 9 shows a cross section through a noninverted double-load model and one through the inverted double-load model that was previously described. The noninverted double-load model illustrates the first-phase delta-top graben buried beneath the second progradational wedge and the second-phase delta-top graben and associated delta-toe fold-thrust belt (Figure 7b, e). The first-phase graben consists of planar regional and strongly listric counterregional extensional growth faults (Figure 9a). The graben infill sediments show strong growth wedges into the counterregional fault system and significant tilting (Figure 9a). In contrast, the second-phase graben system displays a segmented nature with dominantly symmetric geometries and less well formed counterregional fault systems (Figure 9a). The phase 2 graben system is clearly formed on top of the first-phase fold-thrust belt where the underlying ductile polymer was thickest as a result of migration into the cores of anticlinal folds produced by the first phase of differential loading (Figures 7a, 9a). The inverted model (Figure 9b) is characterized by two partially inverted delta-top graben systems with an amplified box fold system at the toe of the second progradational load. Despite unidirectional contraction from the left side of the model, both of these graben systems were reactivated simultaneously.

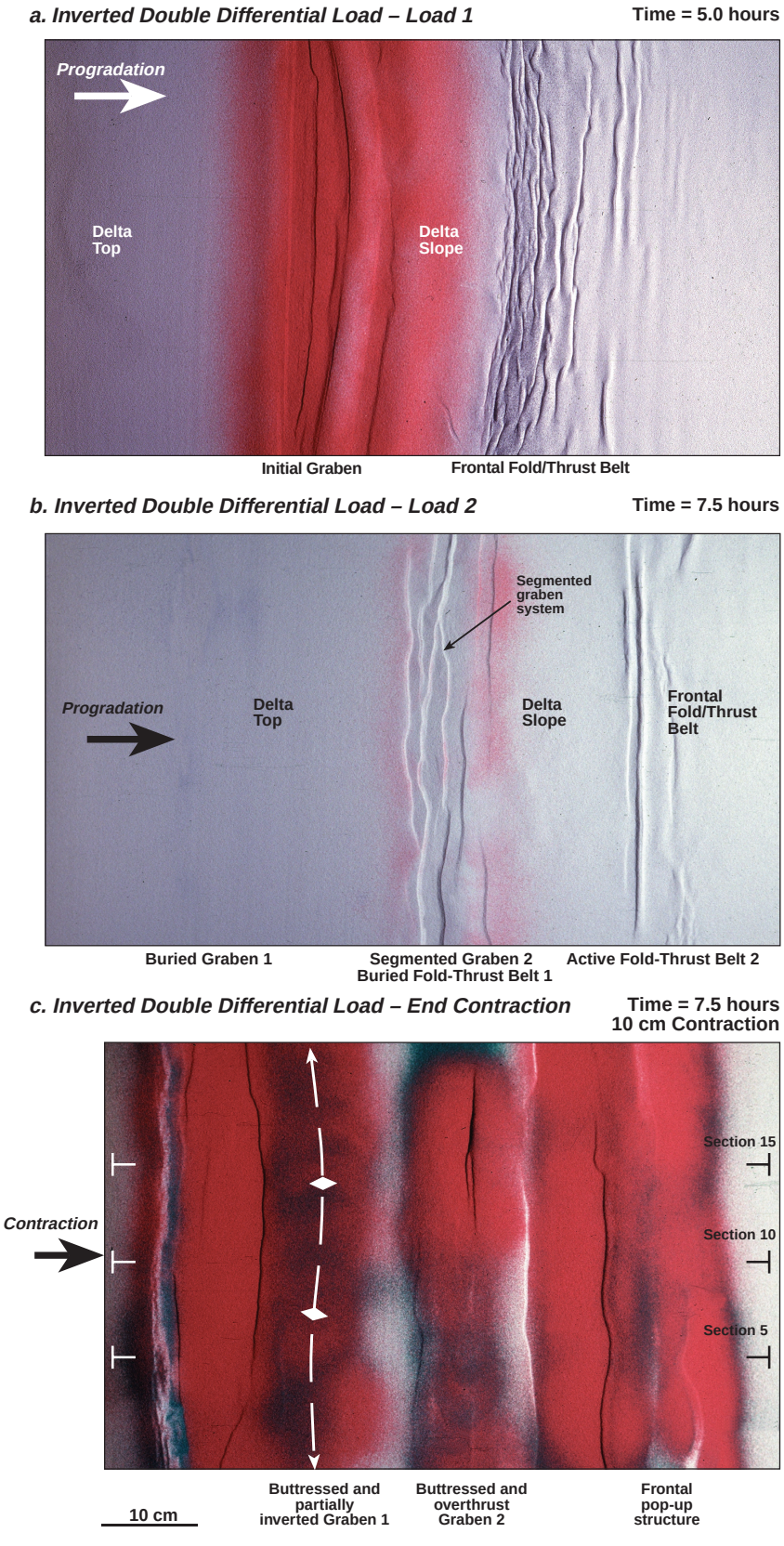


**Figure 7—Model 3 of an inverted double differential load on a ductile substrate. (a) Top shot at the end of load 1. Deformation consists of a delta-top graben and associated fold-thrust belt at the foot of the slope. (b) Top shot at the end of load 2. The delta top has prograded out above the original slope and toe fold-thrust zone. New delta-top graben is heavily segmented due to location above the former fold-thrust belt. (c) Top shot at the end of contraction. The structure mainly consists of major anticlines and intervening synclines. All structures were active simultaneously. (d) Drawing interpreting the top shot at the end of load 2. (e) Interpretation of top shot and the end of contraction.**

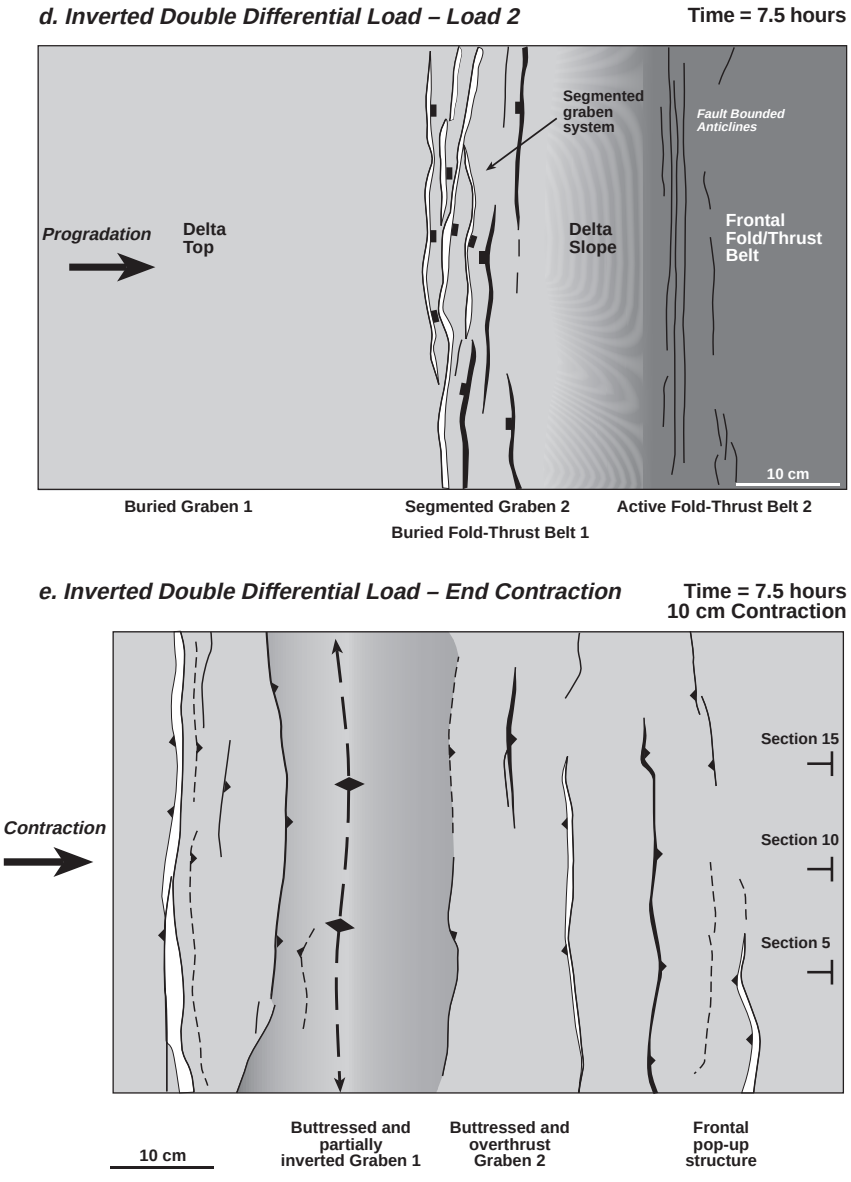


**Figure 7—Continued.**

Figure 10 shows a detailed section and interpretation (section 10, see Figure 7e) of the inverted phase 1 graben system. The first-phase differential loading half-graben systems are characterized by well-developed counterregional listric growth faults (CRF-1 and CRF-2), together with smaller crestal collapse graben faults within the half-graben systems (Figure 10). The larger of the two counterregional faults (CRF-2) has been reactivated and inverted. This inversion, together with a backthrust to counterregional fault CRF-1, has produced an inversion pop-up structure above the phase 1 graben system (Figure 10b). In addition, a number of reactivated extensional faults, new thrusts, and a footwall shortcut fault are associated with the half-graben system of counterregional fault CRF-2. Although there is not total reactivation of the phase 1 extensional fault systems [nor are these to be expected due to the limitations of the analog modeling materials; see the discussion in McClay (1995)], in this model and all of the other duplicate models (cf. Ferguson and McClay, 1997; McClay and Dooley, 1995), the inversion anticlines are always located on preexisting differential load-related extensional half-graben systems and toe-thrust systems.

To simulate the response of an active delta system to far-field contractional stresses, a model was run whereby contraction was imposed while the model still possessed a significant differential load and delta-top extension was active (Figure 11).

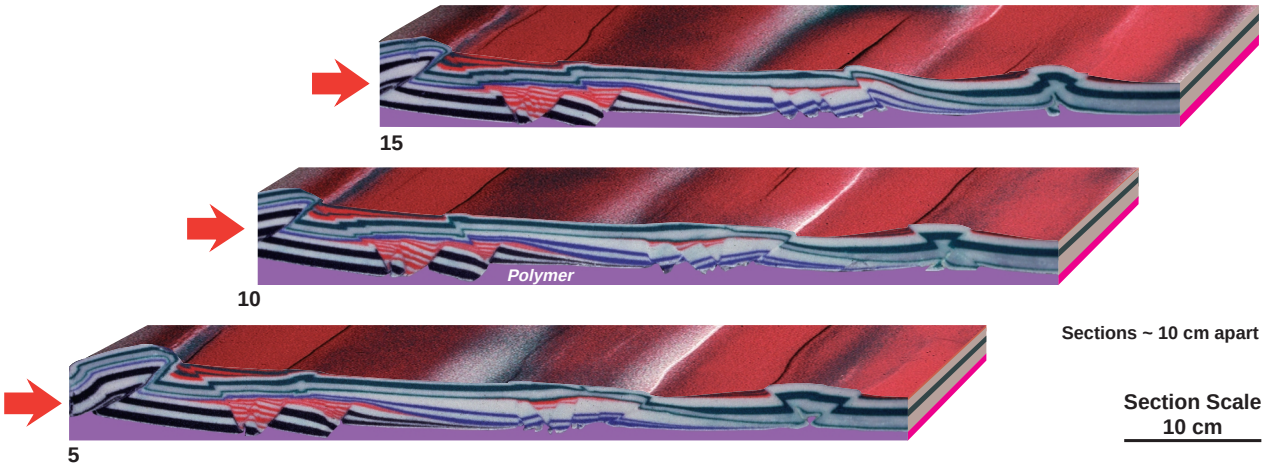


**Figure 8—Three-dimensional reconstruction of the inverted, double differential load experiment. Section lines are indicated on Figure 7c. Major anticlinal features are cored by former delta-top graben. Delta-toe fold-thrust belt has been reactivated as a major pop-up structure.**

Despite significant ongoing contraction, the delta-top graben remained active with significant continued extension, and simultaneously the delta-toe fold-thrust belt was amplified (Figure 11).

## DISCUSSION

### Structural Evolution of the Sanga Sanga Block

The western sections of the Mahakam fold belt in the Sanga Sanga Block are characterized by strongly deformed, tight, fault-bounded anticlines separated by broad synclines. In contrast, the eastern sections show less deformed, open anticlines (Figure 4). Regional and detailed balanced cross section construction and restoration have demonstrated that many of these anticlines, both in the west and in the east, are focused on older early Miocene extensional faults that were reactivated by later shortening (Figures 4, 5). Ferguson and McClay (1997) also showed evidence of inverted extensional faults in the Wain subbasin. Scaled analog models successfully simulated the tectonic development of a progradational delta system and its subsequent contractional deformation (Figures 7–11). These models showed that differential sedimentary loading of a ductile substrate produced linked delta-top graben systems and delta-toe fold-thrust belts (Figure 7a). Second-stage delta loading produced second-stage delta-top extension directly on top of the older first-stage fold-thrust belt as shown by McClay et al. (1998). Contraction of these models, however, produced anticlinal inversion structures formed by reactivation of the buried delta-top graben systems (Figures 7c, 9). This localization of the inversion structures in the physical models agrees with the results of the section restorations across the Sanga Sanga Block, which show that these anticlines are focused on older extensional fault systems detached above and within the overpressured shale sequence (Ferguson and McClay, 1997) (Figure 5). Extensional growth faults have been recognized in many seismic sections offshore Mahakam Delta and, in places, significant reverse faults are also imaged. In particular Malacek and Lunt (1995) showed an excellent seismic example of extensional growth faults that initiated directly on top of an older imbricate thrust system in the offshore part of the Mahakam Delta, similar in style to the analog model results discussed in this paper. Thus, although the inboard, statically loaded portions of the delta underwent inversion and uplift from the middle to the late Miocene, the delta front continued to form depobelts and related delta-toe fold-thrust belts.

The best structural model, therefore, for the evolution of the Mahakam fold belt in the Sanga Sanga Block is that of thin-skinned inverted delta-top graben systems within an overall eastward progradational Mahakam Delta system. Section balancing and restoration shows that the amount of contraction exceeds the amount of extension and that complex, tight, reverse fault-bounded anticlines develop, particularly in the western part of the Sanga Sanga Block (Figure 4). Chambers and Daly (1995, 1997) and Cloke et al., (1997, 1999) proposed a thick-skinned basement-involved inversion model for the northern and western part of the Kutai Basin. There, the basement is closer to surface and is imaged on seismic, and there is not a significant overpressured section above basement. The

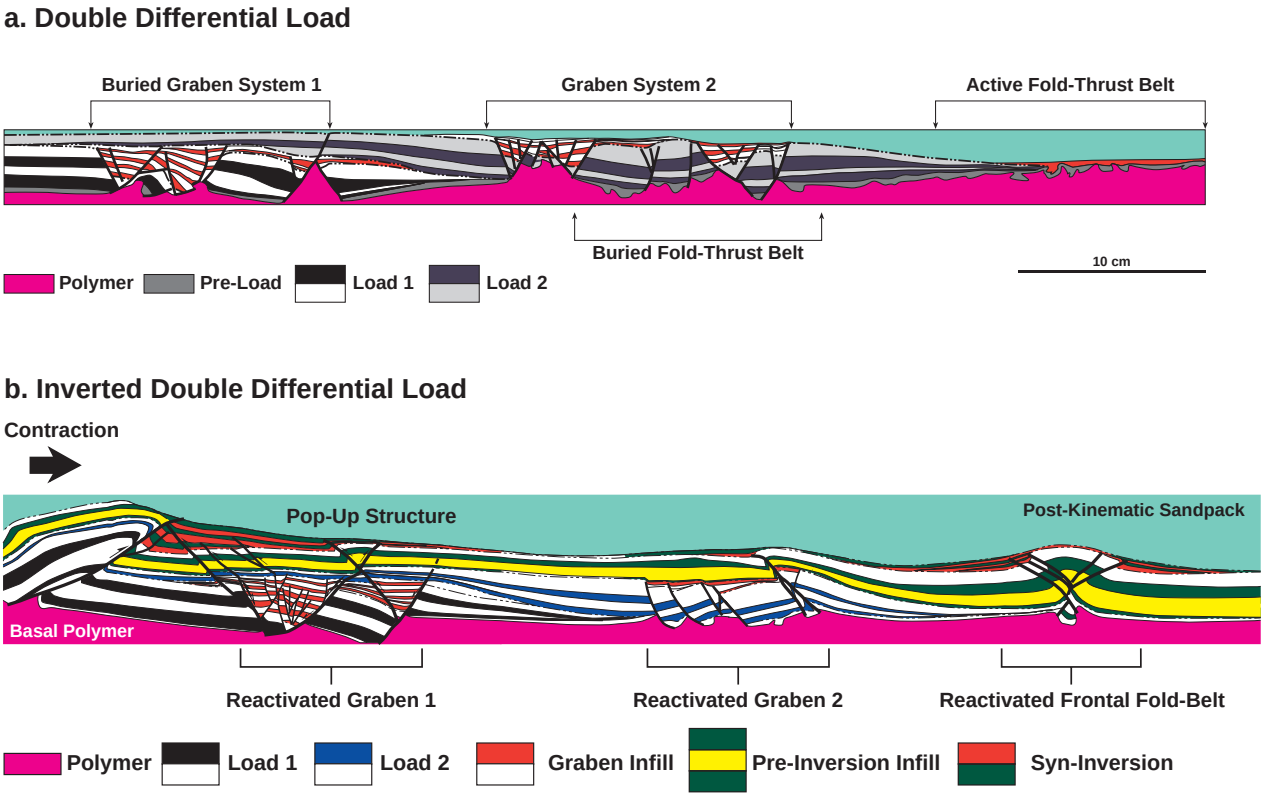


**Figure 9—Line diagram interpretations of cross sections through the models. (a) Double differential load model without inversion. Note the location of the second graben system above the former fold-thrust belt of the initial delta wedge. (b) Double differential load model with inversion. Note that sites of contractional activity during the inversion phase are primarily limited to zones with preexisting structures, i.e., delta-top graben and delta-toe fold-thrust belts.**

model proposed here for the Sanga Sanga Block does not preclude basement-involved inversion below the overpressured zone. The regional uplift on the western parts of the cross sections (Figure 4) and the eastward tilt on the eastern parts of the cross sections may reflect, in part, the influence of deeper basement-involved, inverted Eocene half-grabens, as seen in the northern Kutai Basin (Chambers and Daley, 1995, 1997; Cloke et al, 1997, 1999) where the basement is closer to the surface and imaged on seismic.

## Tectonic Evolution of the Mahakam Fold Belt, Sanga Sanga PSC

It is widely accepted that the Kutai Basin and Makassar Straits initiated with northeast to north-northeast–trending middle–late Eocene rifting following the Late Cretaceous–early Paleocene collision and assemblage of microcontinental fragments, ophiolite obduction, and formation of the Central Kalimantan Mountains (Longley, 1997; Moss et al., 1997). Middle–late Eocene rifting produced initially continental synrift clastics followed by upper Eocene–lower Oligocene deltaic to marine siliciclastics derived from the uplifted terranes to the west (Moss et al., 1997). Recent gravity modeling suggests that the Makassar Straits and the present-day Mahakam Delta are underlain by Eocene oceanic crust (Cloke et al., 1999). The early Miocene through middle Miocene saw the evolution and progressive eastward progradation of the Mahakam Delta system. Northwest-directed contractional deformation in the Sanga Sanga PSC started around 14 Ma (as shown by sequential restoration of the regional cross sections) and continued until the present day, together with continued eastward progradation of the Mahakam Delta system. The inversion probably was caused by the counterclockwise rotation of Borneo, which started at about 20 Ma and continued to about 10 Ma (Hall, 1996, 1997; Moss et al., 1997). At around 14 Ma, extension in the South China Sea ceased and collision of the North Palawan/Reed Bank/Dangerous Grounds Block with Sabah/South Palawan initiating the Palawan Trench A subduction

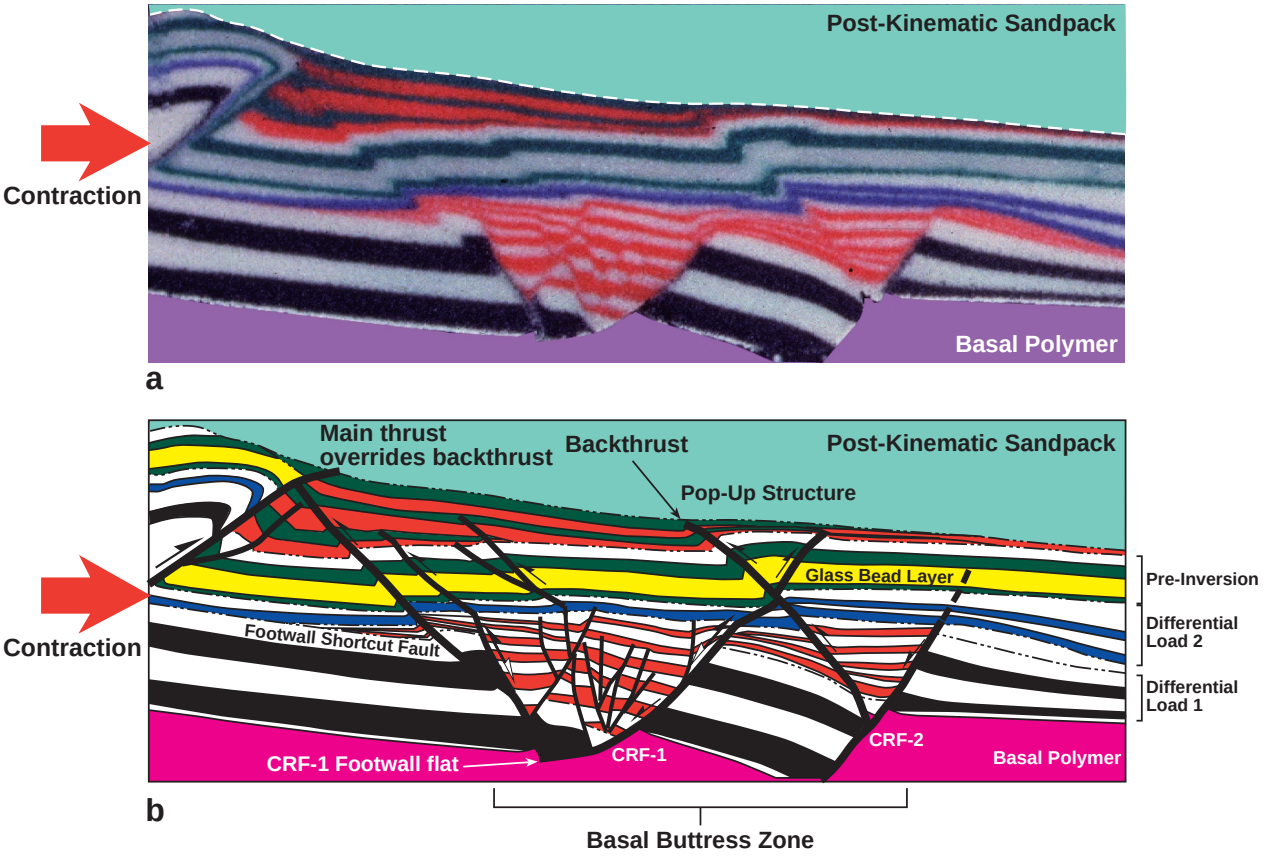


**Figure 10—(a) Detailed cross section and (b) interpretation through an inverted delta-top graben system in the model. See text for further details.**

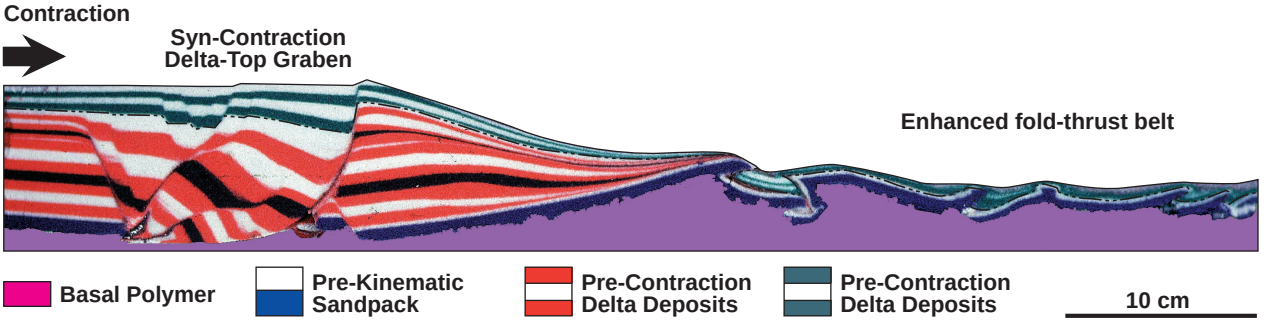


**Figure 11—Cross section through a single differential load where delta-top extension continued during contraction. Contraction was from left to right. Syncontractional sediments are green and white and define an aggradational graben system. During contraction the delta-toe fold-thrust belt was enhanced by a combination of "regional" contraction and contraction due to continued growth of the delta-top graben.**

and northwest-southeast–directed contractional deformation (Metcalfe, 1996; Longley, 1997). During the same period, subduction was occurring in eastern Sulawesi (cf. Hall, 1996, 1997; Moss et al., 1997) culminating in the Banggai-Sulu collision at about 10 Ma. This 10 Ma collision probably gave rise to the accelerated inversion that resulted in amplification and tightening of the Mahakam fold-belt structures. The northwest-directed contractional regime continued to the present day with the collision and

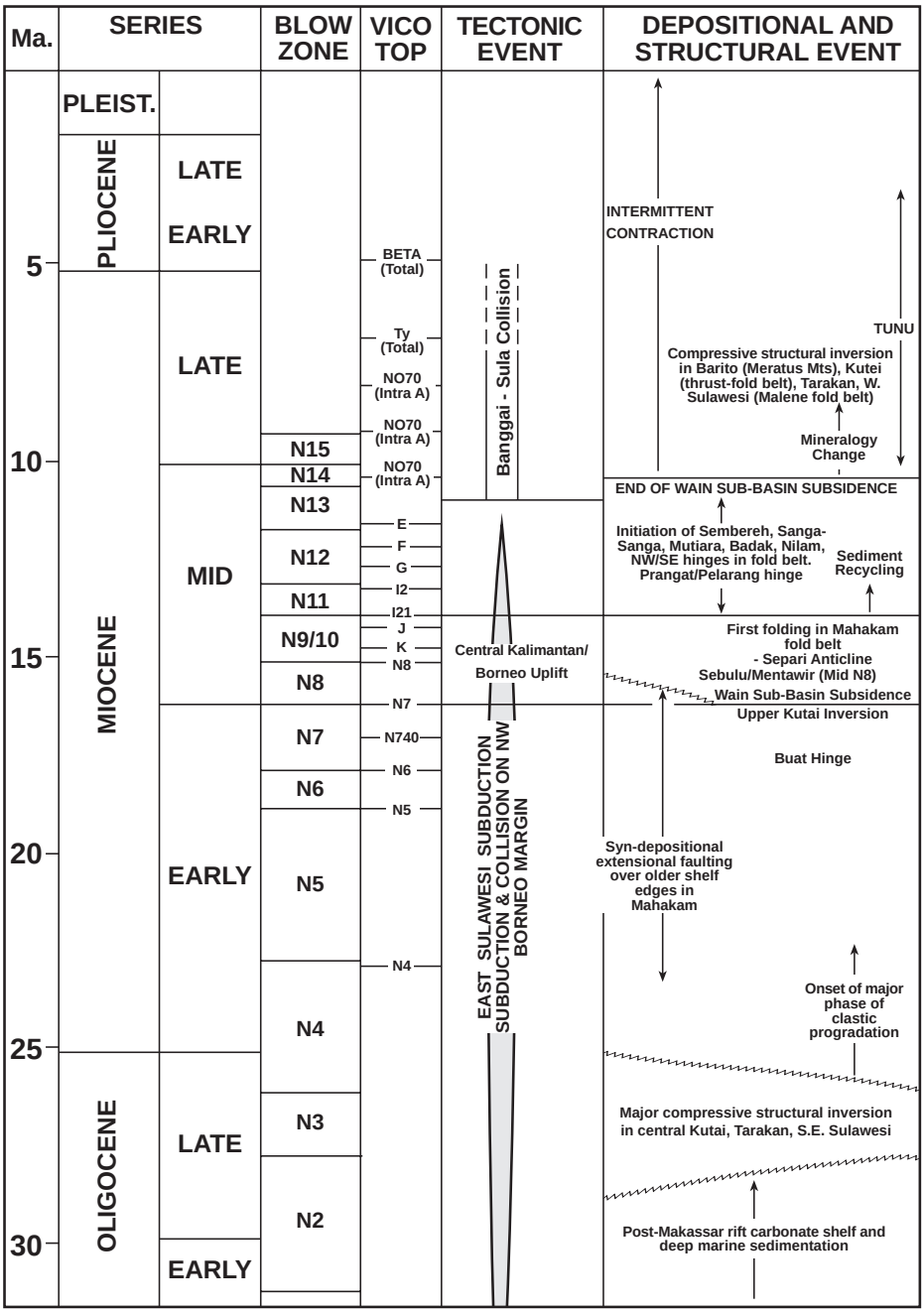


**Figure 12—Tectonic chart showing the timing of depositional and structural events in the Mahakam fold belt.**

continued northward movement of the Indo-Australian plate into the Banda arc. In the Sanga Sanga Block, this contractional deformation from 14 Ma to the present day produced inversion and uplift of the western part of the Mahakam fold belt (as well as in the hinterland of Kalimantan). Figure 12 summarizes the timing and regional tectonic events that have produced the Mahakam fold belt in the Sanga Sanga PSC.

Figure 13 is a synoptic diagram of the preferred model for the detached inversion model for the Sanga Sanga structures. It shows the progressive evolution of the Semberah-Badak-Tunu area through time from approximately 15.7 Ma to the present day. This figure illustrates the sequential, eastward progradation of the Mahakam Delta with the development of extensional growth faults and depobelts near the shelf/slope break, along with delta-toe contractional

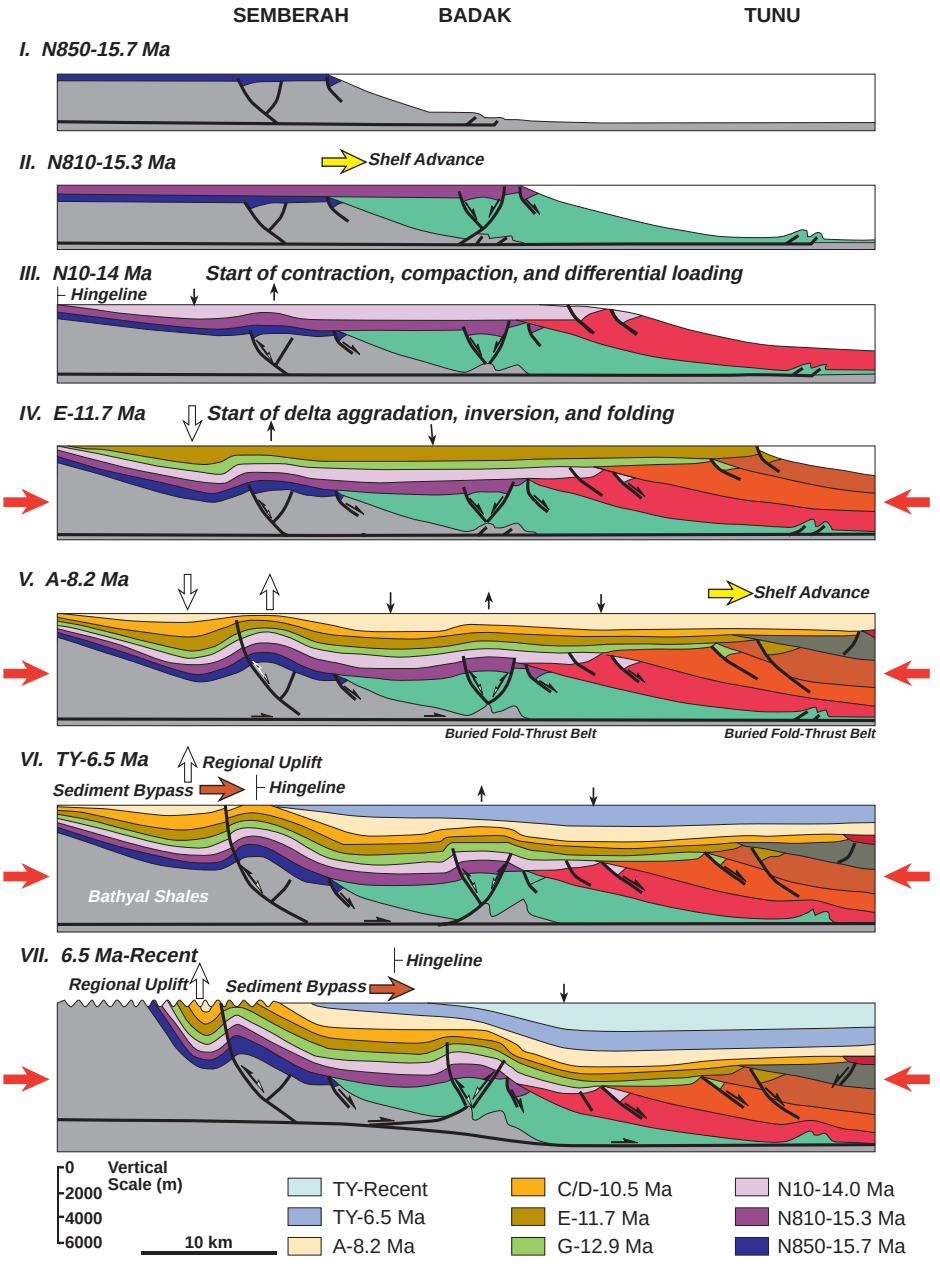


**Figure 13—Synoptic cross sections showing the progressive evolution of the Mahakam fold belt. The location of the Sembereh, Badak, and Tunu fields as indicated on the diagram do not reflect their absolute position or evolution but reflect fields with a decreasing amount of inversion from onshore to offshore.**

structures. Early formed structures were buried by later phases of delta progradation. The structures are detached on the "hard" overpressured prodelta shales that underlie the progradational Mahakam Delta. Contractional deformation from 14 Ma onward produced reactivation and inversion of older extensional faults with most fold amplification and uplift occurring after A deposition (8.2 Ma) (Figure 13). During inversion of the delta progradation continued, burying sections to the east while the western part of the section was uplifted and strongly eroded (Figure 13). Figure 14 shows three-dimensional conceptual models for a progradational delta system (Figure 14a) and an inverted delta system (Figure 14b). Delta-top graben systems (depobelts), bound by regional and counterregional growth faults, form by differential loading that induces shale flowage toward the delta toe, together with the formation of a linked, frontal imbricate fold-thrust belt. Contraction of this system while delta progradation continues produces reactivation of the extensional growth faults to produce detached, uplifted anticlines and

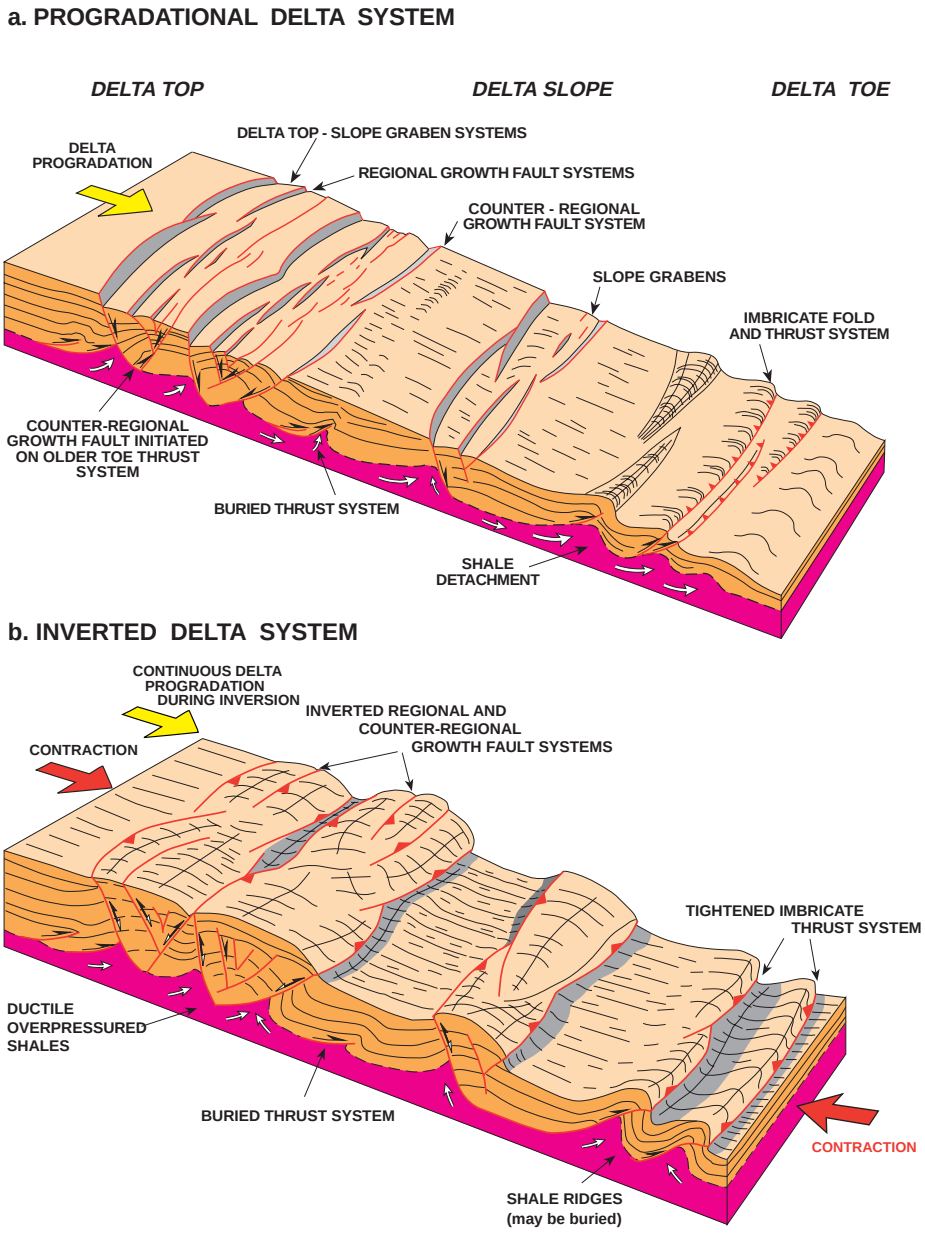


**Figure 14—Schematic synoptic model for progradational delta loading and inversion of progradational delta system. (a) Progradational delta system showing the development of differential load-driven delta-top extensional graben systems and delta-toe contractional fault/fold systems. (b) Inverted delta system showing reactivation and inversion of the delta-top extensional fault systems to produce fault-related anticlines and amplification of the delta-toe fold-thrust belt.**

tightening and amplification of the delta-toe fold-thrust belt (Figure 14b).

Similar detached or thin-skinned delta inversion models may also be applied elsewhere in Borneo. Regional sections through the Barram Delta, Brunei (Schreurs, 1997), also show inverted delta-top depobelts. In particular, high-quality seismic data across the Champion and Seria fields permit imaging of the original delta growth faults, roll-overs, and crestal collapse grabens, but these fields are also uplifted, folded, and eroded by late contraction and inversion (Koopman and Schreurs, 1996). Similarly, in offshore Sabah, Lowell (1995) showed a seismic section across the St. Joseph structure, which can be interpreted as an inverted middle Miocene deltaic growth fault system. The inverted delta model proposed in this paper may also be applicable to other delta systems formed in contractional terranes systems, such as those offshore Trinidad.

## Implications for Petroleum Systems in the Mahakam Fold Belt

Our structural analysis and geometrically and kinematically viable tectonic model for the evolution

of the structures in the Mahakam fold belt in the Sanga Sanga PSC have important implications for the generation, migration, and entrapment of hydrocarbons. The inversion anticlines not only formed the structural traps but also controlled the development of the reservoir channel sandstones (Ferguson and McClay, 1997). Timing of the inversion structures has important implications for generation and migration of petroleum in the Sanga Sanga Block. Paterson et al. (1997) summarized the most recent analyses of the petroleum system of the Kutai Basin and emphasized that middle–late Miocene coals and carbonaceous shales associated with delta-plain to delta-front environments are the source rocks for the Lower Kutai Basin oil and gas fields. These source rocks have total organic carbon contents ranging from 20 to 70% and potential yield of up to 175 mg/g (Paterson et al., 1997). Paterson et al. (1997) defined the top of the hydrocarbon kitchen as being the zone of onset of hydrocarbon expulsion (where $R_o = 0.6$), and the base of the hydrocarbon kitchen is located at the top of the hard overpressure zone (from 3.5–4 km depth in the region of the Nilam field at the present day) (Paterson et al, 1997), which is above the detachment level for the main structures. Vertical seals to the hydrocarbon systems are the delta-plain shales (Paterson et al., 1997), and migration was dominantly lateral, updip into anticlinal and fault-bounded fold traps.

Reservoirs in the Mahakam fold belt are delta-top channel sands deposited in structurally controlled sites (Ferguson and McClay, 1997). In the Badak and Semberah folds (Figure 13), these fluvial channels are parallel to the fold axes deposited either in the hanging walls of extensional growth fault systems or as channels along early formed anticlinal flanks (cf. Ferguson and McClay, 1997). In the Mutiara structure, reservoir channels also occur in the saddle between two growing anticlines (Ferguson and McClay, 1997). Trap formation was early, with fold structures developed by 11.7 Ma and continuing to amplify from 10.5 to 8 Ma. At this stage the kitchen was immature for oil expulsion (Paterson et al., 1997). By 6.5 Ma there was significant structural relief and uplift to the west of the Badak/Nilam structure, and the middle Miocene kitchen intervals were mature. Hydrocarbons migrated out of the synclines into the anticlinal traps at this stage with generation and migration continuing to the present day (Paterson et al., 1997). In general, hydrocarbon migration was updip to the west. Continued inversion and uplift from 6.5 Ma to the present in the western parts of the Sanga Sanga PSC has breached previously formed traps reducing the preservation potential in this part of the Mahakam fold belt.

## CONCLUSIONS

This study has shown that the tight, fault-bounded anticlines and wide synclines that form the Mahakam fold belt on the Sanga Sanga PSC were formed by contractional reactivation and inversion of original, delta-top extensional growth faults. The structures are detached on the underlying overpressured prodelta shale sequence generated by rapid progradational delta loading. In the Sanga Sanga Block, inversion began at approximately 14 Ma and continued to the present day as a result of northwest-directed contraction related to regional collision and subduction northwest of Borneo. Periods of accelerated inversion and anticlinal growth after approximately 10 Ma and 6.5 Ma can be related to key collisions east of Borneo.

A thin-skinned detached inversion model is proposed for the formation of the tight, fault-bounded anticlines in the Sanga Sanga Block. This model involves inversion of differential load-driven, delta-top extensional growth fault systems forming fault-bounded anticlines that become the major hydrocarbon traps in the Sanga Sanga PSC. Scaled analog modeling has shown that this proposed tectonic model is kinematically viable and, in particular, that differential load-driven extension can occur simultaneously with regional contraction. This delta-inversion model can possibly be applied to other terranes where delta systems are subjected to regional contractional deformation.

Our new model for the Sanga Sanga structures involves detached inversion folds above a zone of hard overpressured pro-delta shales and contrasts with other basement-involved inversion models for the Mahakam fold belt structures. Careful section balancing has quantified the amounts of extension and contraction in the Sanga Sanga PSC; moreover, we review the timings of deformation, and in particular, of anticlinal trap formation, which has important implications for the distribution of reservoir sands and for hydrocarbon migration.

## REFERENCES CITED

Bates, J., 1996, Overpressuring in the Kutai Basin: distribution, origin and implications for the petroleum system: Proceedings of the Indonesian Petroleum Association, v. 25, no. 1, p. 93–115.

Bergman, S. C., D. Q. Coffield, J. P. Talbot, and R. A. Garrard, 1996, Tertiary tectonic and magmatic evolution of western Sulawesi and the Makassar Strait, Indonesia: evidence for a Miocene continent-continent collision, *in* R. Hall and D. J. Blundell, eds., Tectonic evolution of southeast Asia: Geological Society of London, Special Publication 106, p. 391–431.

Biantoro, E., B. P. Muritno, and J. M. B. Mamuaya, 1992, Inversion faults as the major structural control in the northern part of the Kutai Basin, East Kalimantan: Proceedings of the Indonesian Petroleum Association 21st Annual Convention, p. 45–68.

Brun, J., D. Sokoutis, and J. Van Den Driessche, 1994, Analogue

modelling of detachment fault systems and core complexes: Geology, v. 22, p. 319–322.
Chambers, J. L. C., and T. E. Daley, 1995, A tectonic model for the onshore Kutai Basin, east Kalimantan, based on an integrated geological and geophysical interpretation: Proceedings of the Indonesian Petroleum Association, v. 24, no. 1, p. 111–130.
Chambers, J. L. C., and T. E. Daley, 1997, A tectonic model for the onshore Kutai Basin, east Kalimantan, *in* A. Fraser, S. Matthews, and R. W. Murphy, eds., Petroleum geology of southeast Asia: Geological Society of London, Special Publication 126, p. 375–393.
Cloke, I. R., S. J. Moss, and J. C. Craig, 1997, The influence of basement reactivation on the extensional and inversion history of the Kutai Basin, eastern Kalimantan: Journal of the Geological Society, London, v. 154, p. 157–161.
Cloke, I. R., S. J. Moss, and J. C. Craig, 1999, Structural controls on the evolution of the Kutai Basin, east Kalimantan: Journal of Asian Earth Sciences, v. 17, p. 137–141.
Daly, M. C., M. A. Cooper, I. Wilson, D. G. Smith, and B. G. D. Hooper, 1991, Cenozoic plate tectonics and basin evolution in Indonesia: Marine and Petroleum Geology, v. 8, p. 2–21.
Ferguson, A., and K. McClay, 1997, Structural modeling within the Sanga Sanga PSC, Kutai Basin, Kalimantan: its application to palaeochannel orientation studies and timing of hydrocarbon entrapment, *in* J. V. C. Howes and R. A. Noble, eds., Proceedings of the IPA Petroleum Systems of SE Asia and Australasia conference: Indonesian Petroleum Association, p. 709–726.
Grundy, R. J., D. W. Paterson, and F. H. Sidi, 1996, Uplift measurements in Tertiary sediments of the Kutai Basin, east Kalimantan, Indonesia, as it relates to VICO Indonesia's PSC and the surrounding area: Society of Exploration Geophysicists Expanded Abstracts, Jakarta International Geophysical Conference, unpaginated.
Hall, R., 1996, Reconstructing Cenozoic SE Asia, *in* R. Hall and D. J. Blundell, eds., Tectonic evolution of southeast Asia: Geological Society of London, Special Publication 106, p. 153–184.
Hall, R., 1997, Cenozoic plate tectonic reconstructions of SE Asia, *in* A. Fraser, S. Matthews, and R. W. Murphy, eds., Petroleum geology of southeast Asia: Geological Society of London, Special Publication 126, p. 11–25.
Hamilton, W., 1979, Tectonics of the Indonesian region: U.S. Geological Survey Professional Paper 1078, 345 p.
Koopman, A., and J. Schreurs, 1996, The coastal and offshore oil and gas fields, *in* S. T. Sandal, ed., The geology and hydrocarbon resources of Negara Brunei Darussalam (2d ed.): Special Publication of the Muzium Brunei and Brunei Shell Petroleum Company Berhad, p. 155–192.
Longley, I. M., 1997, The tectonostratigraphic evolution of SE Asia, *in* A. Fraser, S. Matthews, and R. W. Murphy, eds., Petroleum geology of southeast Asia: Geological Society of London, Special Publication 126, p. 311–340.
Lowell, J. D., 1995, Mechanics of basin inversion from worldwide examples, *in* J. G. Buchanan and P. G. Buchanan, eds., Basin inversion: Geological Society of London, Special Publication 88, p. 39–57.
Malacek, S. J., and P. Lunt, 1995, Sequence stratigraphic interpretation of middle–late Miocene lowstand sands in the Makasar Strait, offshore east Kalimantan, Indonesia (abs.), *in* C. A. Caughy, D. C. Carter, J. Clure, M. J. Gresko, P. Lowry, R. K. Park, and A. Wonders, eds., Proceedings of the international symposium on sequence stratigraphy in southeast Asia: Jarkarta, Indonesian Petroleum Association, p. 355–371.
McClay, K. R., 1990, Extensional fault systems in sedimentary basins. A review of analogue model studies: Marine and Petroleum Geology, v. 7, p. 206–233.
McClay, K. R., 1995, The geometries and kinematics of inverted fault systems: A review of analogue model studies, *in* J. G. Buchanan and P. G. Buchanan, eds., Basin inversion: Geological Society of London, Special Publication 88, p. 97–118.
McClay, K., and T. Dooley, 1995, Structural evolution of the Mahakam fold belt, Kutai Basin, Kalimantan, Indonesia: Report 2 for VICO, Indonesia, 111 p.
McClay, K. R., T. Dooley, and G. Lewis, 1998, Analogue modelling of progradational delta systems: Geology, v. 29, no. 9, p. 771–774.
Metcalfe, I., 1996, Pre-Cretaceous evolution of SE Asian terranes, *in* R. Hall and D. J. Blundell, eds., Tectonic evolution of southeast Asia: Geological Society of London, Special Publication 106, p. 97–122.
Moss, S. J., and J. L. C. Chambers, 1999, Tertiary facies architecture in the Kutai Basin, Kalimantan, Indonesia: Journal of Asian Earth Sciences, v. 17, p. 157–182.
Moss, S. J., J. Chambers, I. Cloke, A. Carter, D. Satria, J. R. Ali, and S. Baker, 1997, New observations on the sedimentary and tectonic evolution of the Tertiary Kutai Basin, east Kalimantan, *in* A. Fraser, S. Matthews, and R. W. Murphy, eds., Petroleum geology of southeast Asia: Geological Society of London, Special Publication 106, p. 395–417.
Ott, H. L., 1987. The Kutai Basin: a unique structural history: Proceedings of the Indonesian Petroleum Association 16th Annual Convention, p. 307–316.
Packham, G., 1996, Cenozoic SE Asia: reconstructing its aggregation and reorganization, *in* R. Hall and D. J. Blundell, eds., Tectonic evolution of southeast Asia: Geological Society of London, Special Publication 106, p. 123–152.
Paterson, D. W., A. Bachtiar, J. A. Bates, J. A. Moon, and R. C. Surdam, 1997, Petroleum systems of the Kutai Basin, Kalimantan, Indonesia, *in* J. V. C. Howes and R. A. Noble, eds., Proceedings of the IPA petroleum systems of SE Asia and Australasia conference: Jarkarta, Indonesian Petroleum Association, p. 709–726.
Schreurs, G., 1997, The petroleum geology of Negara Brunei Darussalem; an update, *in* J. V. C. Howes and R. A. Noble, eds., Proceedings of the IPA petroleum systems of SE Asia and Australasia conference: Jarkarta, Indonesian Petroleum Association, p. 751–766.
Syarifuddin, N., and I. Busono, 1999, Regional stress alignments in the Kutai Basin, east Kalimantan, Indonesia: a contribution from a borehole breakout study: Journal of Asian Earth Sciences, v. 17, p. 123–136.
van de Weerd, A. A., and R. A. Armin, 1992, Origin and evolution of the Tertiary hydrocarbon-bearing basins in Kalimantan (Borneo), Indonesia: AAPG Bulletin, v. 76, p. 1778–1803.
Weijermars, R., M. P. A. Jackson, and B. Vendeville, 1993, Rheological and tectonic modelling of salt provinces: Tectonophysics, v. 217, p. 143–174.
Williams, G., and I. Vann, 1987, The geometry of listric normal faults: deformation in their hanging walls: Journal of Structural Geology, v. 9, p. 789–793.

## ABOUT THE AUTHORS

### Ken McClay

Ken McClay is a native of Adelaide, South Australia. He graduated with a B.Sc. (honors) degree from Adelaide University. He subsequently undertook an M.Sc. degree in structural geology and rock mechanics at Imperial College, University of London, where he also obtained a Ph.D. in structural geology in 1978. He lectured at the University of London Goldsmiths College until 1986, when he moved to Royal Holloway University of London. He has been professor of structural geology since 1991, and is director of the fault dynamics research group. His research involved the study of extensional, thrust, strike-slip, and inversion terranes and their applications to hydrocarbon exploration. He has published widely, consults, and offers short courses to industry.

### Tim Dooley

Tim Dooley, a native of Waterford, Ireland, graduated with a B.A. (mod.) degree from Trinity College, Dublin, Ireland, in 1988. He subsequently undertook a Ph.D. in structural geology at Royal Holloway University of London. Since 1994, Tim has been a postdoctoral research assistant with the fault dynamics research group. His current research interests include analog modeling of strike-slip faults, salt, shale, and compressional tectonics, as well as developing graphic and interactive techniques for presenting these data to students and industry. His work with the fault dynamics research group includes preparing and presenting short courses to industrial sponsors.

### Angus Ferguson

Angus Ferguson received a B.Sc. degree in geology from the University of Waterloo, and an M.Sc. degree in geology and then a B.Sc. degree in geophysics from the University of Calgary, Alberta, Canada. He worked as an explorationist for 20 years in Canada and Indonesia, and has eight years experience in exploration in the Mahakam Delta area. Currently he is an independent consultant in seismic and geological interpretation, in addition to teaching field seminars on the application of sequence stratigraphy, structural geology, and sedimentology to exploration.

### Josep Poblet

Josep Poblet gained a geology degree in 1986 from the University of Barcelona, where he also completed an M.Sc. and a Ph.D. on the geology of the Pyrenees. Between 1992 and 1996, he undertook two postdoctoral fellowships at Royal Holloway University of London, and the University of Barcelona. His research was mainly concerned with modeling thrust-related folds and tectonics-sedimentation relationships. Currently, Josep is a lecturer at the University of Ovideo, Spain.